Electrical Supplementary Information

Title: Self-aligned synthesis of NiPt@Pt_{shell} nanocrystal with contrivable heterojunction structure and oxygen reduction activity

Authors: Tsan-Yao Chen,[a,b*†] Sun-Tang Chang,[c] Chih Wei Hu,[a] Yen-Fa Liao,[c] Ying Jhen Sue,[d] Yang-Yang Hsu,[a] Kaun-Wen Wang,[e] and Yu-Ting Liu[d*†]

Affiliations:

[a] Department of Engineering and System Science, National Tsing Hua University, Hsinchu 30013, Taiwan

[b] Institute of Nuclear Engineering and Science, Hsinchu 30013, Taiwan

[c] National Synchrotron Radiation Research Center, Hsinchu 30076, Taiwan

[d] Department of Soil and Environmental Science, National Chung Hsing University, Taichung 402, Taiwan.

[e] Institute of Materials Science and Engineering, National Central University, Taiwan

*To whom correspondence should be addressed:

Tsan-Yao Chen, email: chencaeser@gmail.com Tel: +886-3-5715131#34271;

Yu-Ting Liu, email: yliu@nchu.edu.tw

1. The electrochemical analysis on MOR activity and durability of experimental NiPt@Pt NC

The electrolyte for the MOR sweeping experiments are given here:

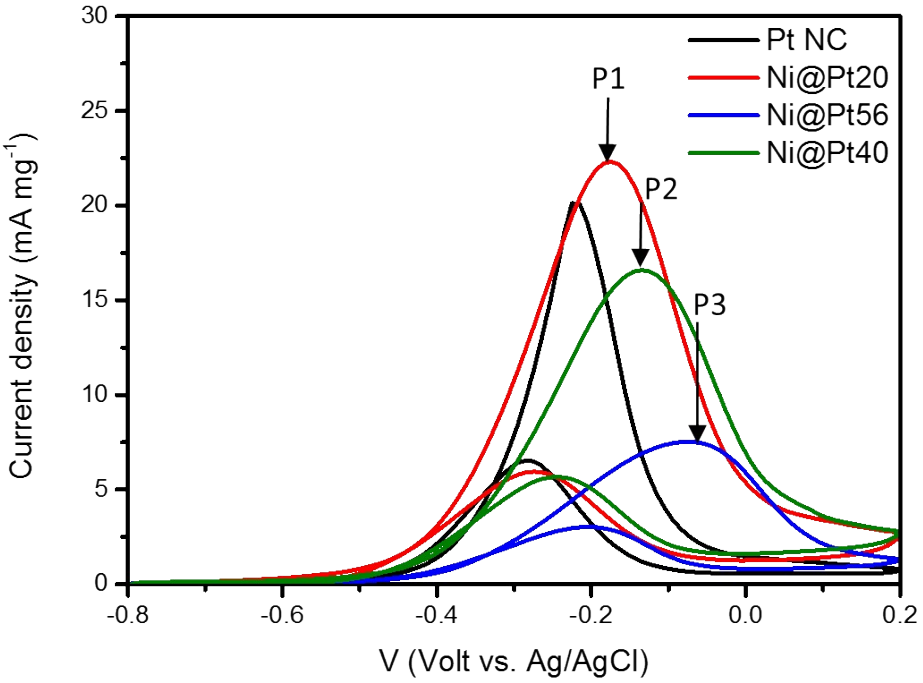

Fig. S1. The cyclic voltammetry sweeping curves for methanol electrooxidation reaction on NiPt@Pt NC compared with Pt NC.

The electrolyte for MOR reaction is the aqueous solution of 1.0M methanol and NaOH mixture. The scan rate for the potential sweep was set to be 20 mVs^{-1}.

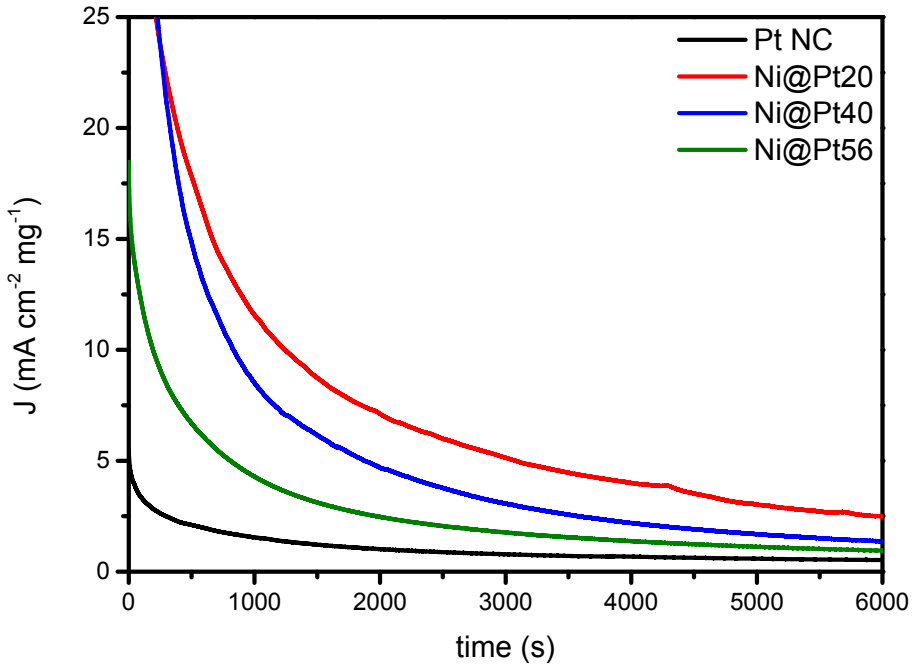

Fig. S2 long-term MOR reaction current vs. time curves for the experimental NiPt@Pt NC compared with Pt NC.

The CO poisoning tolerance and the structure stability of the two types of NCs can be elucidated by the retained current density at long-term AC curves. It is interesting to note that the activity of Ni@Pt20 is 10.1-folds higher than that of Pt NPs after the long-term MOR measurement for 6000s indicating their superior CO tolerance and electrochemical stability. Therefore, the poor anti-CO capability could also be one of the main causes for the sudden current drop of Pt NPs in the first 100 second of AC curve. In addition, the current drop rate is progressively decreased suggesting the enhancing structure stability of Ni@Pt NCs with decreasing Pt content till 20 at%.

Table S1. The summarized results of electrochemical surface area (ECSA) and mass activity (MA) of experimental NCs.

sample	QDH [C] * 100	ECSA	MA
Pt NPs	7.92E-03	37.72	-0.65
Ni@Pt20	5.74E-03	27.35	-1.32
Ni@Pt40	3.76E-03	17.89	-0.67
Ni@Pt56	3.56E-03	16.96	-0.46

The electrolyte is the aqueous solution of 1.0M $HClO_4$. Potential scan rate is 20mV s^{-1}.

2. X-ray photoemission spectroscopy analysis of NiPt@Pt NC

The Pt/Ni ratios of NiPt@Pt NC are determined by dividing the areas of Pt 4f emission peaks by the sum of Ni 3s and Pt 4f emission peaks with the consideration of corresponding photon cross section and emission efficiency. The chemical ratios of Pt/Ni are determined at an excitation energy of 650 eV (kinetic energy of photoelectron is 580 eV corresponding to a mean free path of 8~10 Å). It refers to the probing depth of 24~30 Å (the scheme for XPS probing depth for Ni@Pt20, Ni@Pt40, and Ni@Pt56 are shown in Fig. R2). The XPS spectra and fitting results are given in Fig. S3 and Table S2. From SAXS analysis (Table 1), we notice that the shell crystal thickness is ranged from 9 to 30 Å which is about the same to the probing depth of XPS. Therefore, XPS results illustrate the chemical composition near interface for Ni@Pt20, Ni@Pt40 and near surface region for Ni@Pt56. Accordingly, the Pt/Ni ratio is 1.19 for Ni@Pt20, 2.18 for Ni@Pt40, and 10.46 (or higher) for Ni@Pt56.

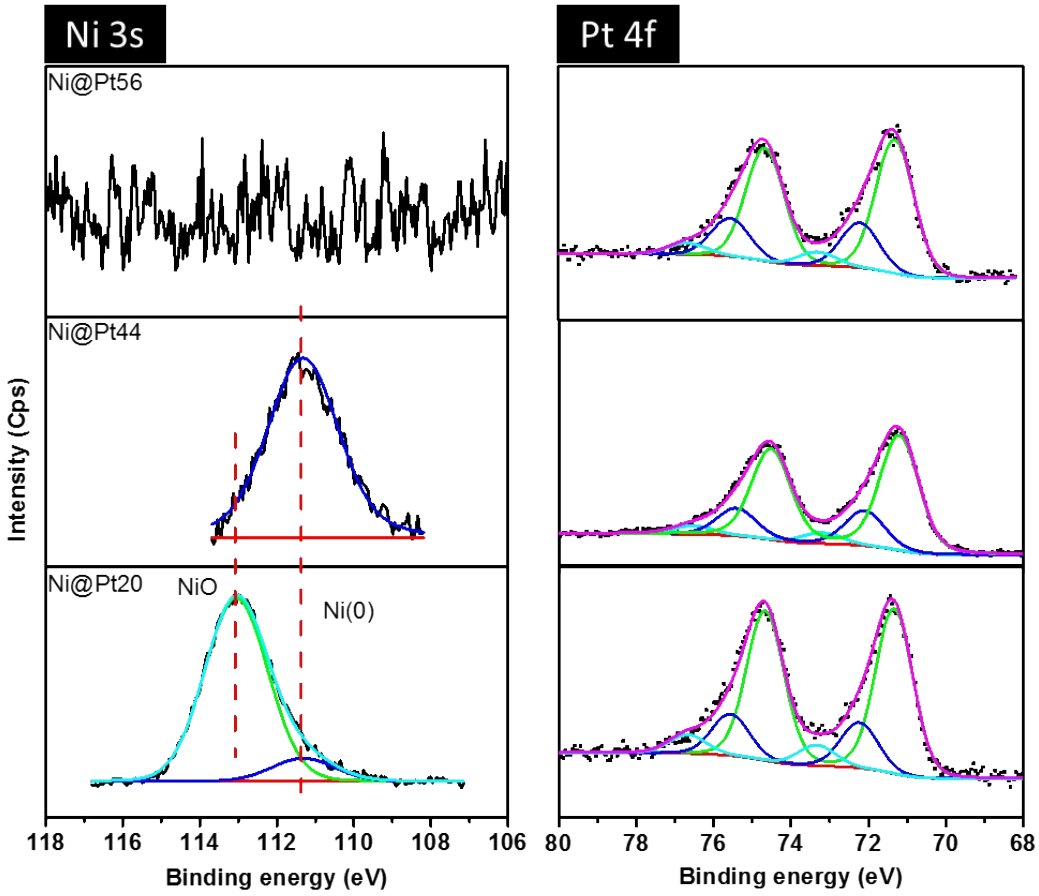

Fig. S3 Ni 3s and Pt 4f XPS spectra of Ni@Pt20, Ni@Pt40, and Ni@Pt56 NC.

Table S2 XPS determined chemical composition of NiPt@Pt NCs

	Ni@Pt20	**Ni@Pt40**	**Ni@Pt56**	
Area from Pt4f : Ni3s	(137365/115348) =1.19:1	(146680/67192.7) =2.18:1	(168217/X) =X	(15623.8/1492.04) =10.46:1 (from survey)

3. Electrochemical analysis

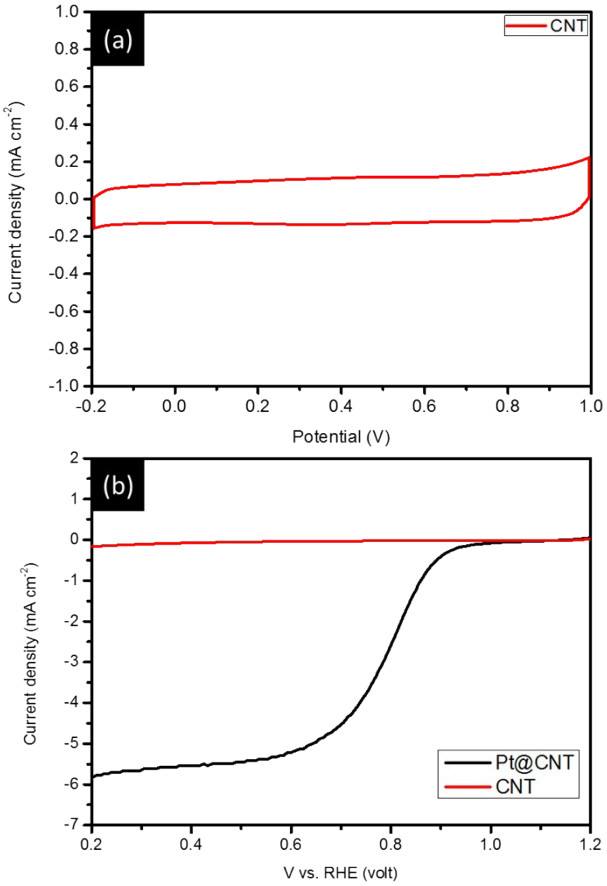

Fig. S4 (a) CV curve of CNT sample in a N_2 purged $HClO_{4(aq)}$ solution (0.5 M) and (b) LSV curves of CNT and Pt@CNT samples in a O_2 purged $HClO_{4(aq)}$ solution (0.5 M).

Fig. S4a demonstrates the CV sweeping curve of CNT sample in a N_2 purged $HClO_{4(aq)}$ solution (0.5 M), the conditions for CV experiment are identical to that are utilized in this study. As clearly indicated, CNT sample possesses a good squareness across the entire CV curve which is a typical feature of super-capacity in electrolyte. In this CV sweep curve, the redox reaction peaks are indistinct implying the inert oxygen reduction activity (as well as low oxidation state) in CNT surface.

Fig. S4b compares the LSV spectra of CNT and Pt@CNT samples. As depicted, the changes of current density is indistinct on CNT with potential decreased from 1.2 to 0.2 volt. The current intensity of CNT is -0.025 mA cm^{-2} at 0.85 volt (~2% to that of Pt@CNT) which is nearly inactivate to oxygen reduction as compared to CNT supported NC.